Measurements of brain activity complexity for varying mental loads

Mukeshwar Dhamala,[1,2] Giuseppe Pagnoni,[2] Kurt Wiesenfeld,[1] and Gregory S. Berns[2,3]

[1]*School of Physics, Georgia Institute of Technology, Atlanta, Georgia 30332*
[2]*Department of Psychiatry and Behavioral Sciences, Emory University, Atlanta, Georgia 30322*
[3]*Department of Biomedical Engineering, Georgia Institute of Technology, Atlanta, Georgia 30332*

Using functional magnetic resonance imaging, we investigate the variation in dynamical complexity of human brain activity for different mental loads. Our experiments measured the activity of ten subjects under three experimental conditions: a rest condition, a periodic task of finger opposition, and a task of finger opposition alternated with mathematical serial calculation. We used the correlation dimension to gauge the spatiotemporal complexity of brain activity. The experiments show a direct relationship between this complexity and the difficulty of the task. A natural interpretation is that higher levels of mental load recruit a larger number of independent neural processes that contribute to complex brain dynamics. These results suggest the possibility that the relative change in correlation dimension can be a useful global measure of brain dynamics, e.g., in determining the levels of mental activity, even if little is known about the underlying neurological processes.

I. INTRODUCTION

The correlation dimension has been used widely in the analysis of experimental time series, including data from biological systems [1,2] since its introduction by Grassberger and Procaccia [3]. In particular, it has been a useful global measure in the analysis of human electroencephalogram (EEG) data [4–8]. The complexity of electrical activity in the brain is reported to correlate with global changes in mental state [9–11]. Theoretical models have also been proposed predicting that automatic behavior reflects processes of lower complexity than those underlying consciously controlled behavior (see Ref. [12]).

From its inception, functional magnetic resonance imaging (FMRI) has been a powerful experimental tool for monitoring spatiotemporal brain activity, with a wealth of new opportunities to advance our understanding of brain organization. Modern time series analysis provides natural concepts for exploring spatiotemporal complexity of the sort observed in FMRI studies. In this paper, we report the variation of the correlation dimension from FMRI signals of the human brain subject to different mental loads. The results demonstrate that an increased mental load yields FMRI signals of greater dynamic complexity. This has a natural interpretation that higher levels of mental activity are associated with a larger number of independent neural processes that contribute to complex brain dynamics.

The FMRI signal, known as the blood-oxygen-level-dependent (BOLD) contrast, represents the magnetic susceptibility variation associated with neural activity [13,14]. A local neuronal excitation results in a regional increase in the oxygen consumption followed by a change in cerebral blood flow. This vascular overcompensation increases the net oxygenation of venous blood, which is paramagnetic in its deoxygenated state while other tissue components as well as oxygenated blood are diamagnetic. The increase in blood oxygenation of venous blood reduces the susceptibility induced signals. The FMRI signals are thus dependent on the underlying neuronal activity, the hemodynamics of the brain, and the imaging physics and yield a typical spatial resolution of a few millimeters and with a temporal resolution of a few hundred milliseconds. To the first approximation, one can think of the observed BOLD signals of FMRI as a smoothed version of the underlying neural activity.

The experiments reported here were designed to test the hypothesis that more difficult mental tasks are associated with more dynamically complex FMRI signals. We set up three experimental conditions: a reference condition (rest), a task of periodic finger opposition (finger tapping), and another task of periodic finger opposition alternated with mathematical calculation. These three tasks were selected to span a range of mental complexity, ranging from minimal (rest) to high (mathematical calculation). The complexity of the corresponding spatiotemporal time series was analyzed by computing the correlation dimension. Because of certain practical limitations concerning the length and resolution of the acquired data, we used a modified algorithm to estimate the correlation dimension that takes advantage of the multiplicity of time series inherent in the spatially resolved images.

This paper is organized as follows. Section II contains a summary of the essential parts of the modified Grassberger-Procaccia (GP) algorithm for correlation dimension estimates from multiple time series. In Sec. III we describe the experimental setup and results. In Sec. IV we discuss the physiological interpretation of these results and outline a few open problems that, if overcome, would substantially enhance the use of complexity measures for future FMRI studies.

II. BACKGROUND

In this section we briefly summarize the procedure for generating correlation dimension estimates from spatiotemporal time series. We also contrast this approach with the linear imaging analysis more conventionally used in FMRI brain studies.

Principal Component Analysis (PCA), also known as the Karhunen-Loéve transformation, Singular Value Decomposi-

tion (SVD) or Empirical Orthogonal Functions, is a common method to reduce the dimensionality and to extract important modes of activity from massive datasets, for example FMRI data from the human brain. Implementation of PCA amounts to a search for the direction of maximum variance in the dataset, followed by an orthogonal projection of data onto a subspace spanned by the direction vectors with highest variance. It has been indicated that PCA can extract qualitatively nonlinear dynamical features from experimental time series [15–17]. PCA is easily implemented by the singular value decomposition of the data matrix.

A singular value decomposition of $M \times N$ real matrix $\mathbf{A}$ is any factorization of the form $\mathbf{A} = USV^T$, where U is an $M \times M$ orthogonal matrix, V is an $N \times N$ orthogonal matrix, and S is an $M \times N$ diagonal matrix with $S_{ij} = 0$ if $i \neq j$ and $S_{ii} = \sigma_i \geq 0$, i.e., with leading diagonal elements $\sigma_1 \geq \cdots \geq \sigma_r \geq 0$, r being min(M,N). The σ_i are the singular values, and the first r columns of U and V are the left and the right singular vectors, respectively. In the context of a spatiotemporal data matrix, such as FMRI data, U captures the temporal and V^T the spatial information from the data matrix $A_{M \times N}$, where M is the number of time points and N the number of voxels (volume elements, i.e., sources of FMRI signals). To represent the amount of independent contribution in the total variance of the data by each component, we assign the normalized eigenvalues of S, i.e., $\sigma_i^2 / \Sigma_{i>1} \sigma_i^2$, as the weighting factors to the temporal components in the matrix U. Taking the first few principal components weighted with these factors will reduce the noise level while preserving the correct phase dynamics in the reconstructed space.

The Grassberger-Procaccia algorithm is based on an appropriate phase-space reconstruction. The time-delay embedding is one popular method. Given a scalar time series $s(t)$, one forms a sequence of vectors $\mathbf{x}(t) = (s(t), s(t+\tau), \ldots, s(t+[m-1]\tau)$, where m is the embedding dimension and τ is the delay time. Under mild assumptions about the underlying dynamics, the nature of the measurement function that produces $s(t)$, and the choice of τ, it can be shown that various dynamical quantities of the reconstructed set are the same as those of the underlying attractor, provided that m is suitably large [18,19]. In particular, if the correlation dimension of the underlying attractor is D_2, then $m \geq D_2$ allows one to determine D_2 from an embedding of a corresponding time series [20], and $m \geq 2D_2 + 1$ suffices to produce a diffeomorphism between the embedded set and the underlying attractor under mild assumptions [19].

Grassberger and Procaccia [3] have shown that D_2 can be evaluated by using the correlation integral $C(\epsilon)$, which is defined to be the probability that a pair of points chosen randomly with respect to the natural measure is separated by a distance less than ϵ on the reconstructed set. For a trajectory of length N, the correlation integral can be approximated by the sum,

$$C_N(\epsilon) = \frac{2}{N(N-1)} \sum_{j=1}^{N} \sum_{i=j+1}^{N} \Theta(\epsilon - \|\mathbf{x}_i - \mathbf{x}_j\|), \quad (1)$$

where Θ is the Heaviside function $[\Theta(x) = 1$ if $x \geq 0$ and $\Theta(x) = 0$ otherwise], and $\|\cdot\|$ denotes a suitable vector norm,

say $\|\mathbf{x}\| = \max\{\|x_i\| : 1 \leq i \leq m\}$. For large N, the correlation dimension D_2 is given by

$$D_2 = \lim_{\epsilon \to 0} \lim_{N \to \infty} \frac{d \log_2 C_N(\epsilon)}{d \log_2 \epsilon}. \quad (2)$$

Thus for a single long time series, once the embedding vectors are reconstructed, the estimation of the correlation dimension is done in two steps. First, one has to determine the correlation sum $C(\epsilon)$ for the range of ϵ available and for several embedding dimensions m. Then, for a given value of m, one looks for a plateau in the plot of $d \log_2 C(\epsilon)/d \log_2 \epsilon$ versus $\log_2 \epsilon$ to estimate the value of D_2. The presence of a plateau indicates self-similar structure known as fractal [21]. Data collected at a high sampling rate usually contain temporal correlations in the phase space that presents a bias in the calculation of the correlation sum. In that case, it is suggested that the points that are too close in time need to be discarded, which is known as the Theiler correction [22].

Multiple time series, for example, spatiotemporal series, can be assumed to be either independent realizations of the same observable in a given system or different observables of a single attractor measured simultaneously. The Grassberger-Procaccia algorithm can be easily adapted for multiple time series by separately embedding each time series and, in the correlation sum, by counting the pair of points (from all the series) that fall inside a hypersphere of radius ϵ around the center. Thus, for multiple series, the correlation sum can be written as

$$C_{N_T}(\epsilon) = \frac{2}{N_T(N_T-1)} \sum_{j=1}^{N_T} \sum_{i=j+1}^{N_T} \Theta(\epsilon - \|\mathbf{X}_i - \mathbf{X}_j\|), \quad (3)$$

where $N_T = N_1 + N_2 + \cdots + N_K$ and $\mathbf{X}$ is the set of all the delayed vectors, i.e, $\{\{\mathbf{x}_i^1\}_{i=1}^{N_1}, \{\mathbf{x}_i^2\}_{i=1}^{N_2}, \ldots, \{\mathbf{x}_i^K\}_{i=1}^{N_K}\}$, where $\mathbf{x}_i^{(1,2,\ldots,K)}$'s are the delay vectors constructed from individual time series. Here $N_1, N_2, \ldots$ are the numbers of delayed vectors in the reconstructed space from K number of time series. In this reconstructed space of delay vectors $\mathbf{X}$, the correlation sum, as defined in Eq. (3), measures the probability that a randomly selected pair of delay coordinate points from the vector set $\mathbf{X}$ is separated by a distance less than ϵ. D_2 is then determined from the converging plateaus (corresponding to different m) in the plot of $d \log_2[C_{N_T}(m,\epsilon)]/d \log_2(\epsilon)$ vs $\log_2(\epsilon)$ by the similar procedure as defined by Eq. (2). This sum from multiple series is known as the cross correlation sum and can be used as the measure of overlap of multiple time series [23]. Although a fundamental mathematical understanding is lacking, the validity of the phase-space reconstruction from multiple series has been checked with mathematical models [24,25]. Research reporting improved results for correlation dimension and density estimates with multiple channel EEG data [4,26] also support the applicability of this scheme for multiple time series. With some normalization scheme, the dimension density can be defined as [27]

$$\rho(\epsilon, m) = \frac{d \log_2 C_{N_T}(m,\epsilon)/m}{d \log_2 C_{N_T}(1,\epsilon)} \quad (4)$$

and then the correlation dimension is just $m\rho(\epsilon,m)$ at the scaling regions.

III. FMRI EXPERIMENT AND RESULTS

Ten normal, right-handed subjects (five males and five females), aged between 23 to 36, participated in this study.[1] Subjects were asked to perform three different tasks during three functional runs of FMRI. These experimental tasks were: (i) rest (reference condition), (ii) rest alternated with finger opposition, and (iii) mathematical calculation alternated with finger opposition. The order of these tasks presented was randomized across subjects. In the first task (reference condition), subjects were asked to relax and rest in the scanner for 500 scans (500 s). The second task consisted of twenty-five epochs of rest alternated with finger opposition (10 s each). With visual instructions on a screen, subjects were asked to rest and to tap their index fingers to their thumb on the right hand in periodic cycles for about 500 s. The final task was 25 cycles of mathematical calculation alternated with finger opposition. The mathematical calculation involved successive subtractions of 17 from a random three-digit number. We hypothesized that these tasks would present an increasing mental load resulting in an increasing degree of complexity of FMRI signals and that the complexity would be different enough to be captured in correlation dimension estimates.

All imaging was performed on a Philips 1.5 T Intera instrument. Each imaging session consisted of a scout image, a T1-weighted structural scan, and three runs of 500 scans each in the functional sessions. Each functional scan was acquired with eight slices each with 8 mm thickness and orientation of slice planes of about 10° down from the anterior commissure–posterior commissure line [echo-planar imaging, gradient-recalled repetition time (TR)=1000 ms, echo time (TE)=40 ms, flip angle=81°, 64×64 matrix].[2] This imaged a major portion of the brain comprising areas of hypothesized motor and cognitive activations. Before the extraction of principal components, each functional run was corrected for head of subjects movement using a 6 degrees of freedom rigid-body transformation as implemented in the software package called SPM99 [28].

We used singular value decomposition to reduce the FMRI data from a large number of signal sources (8×64 $\times64$ voxels) into a few dominant modes of spatiotemporal activity. Each temporal component of SVD (U as defined in Sec. II) had 500 data points that evolved in time as the signals were sampled at 1 Hz. We extracted a number of components from the FMRI data and used 50 properly weighted components that accounted for more than 96% residual vari-
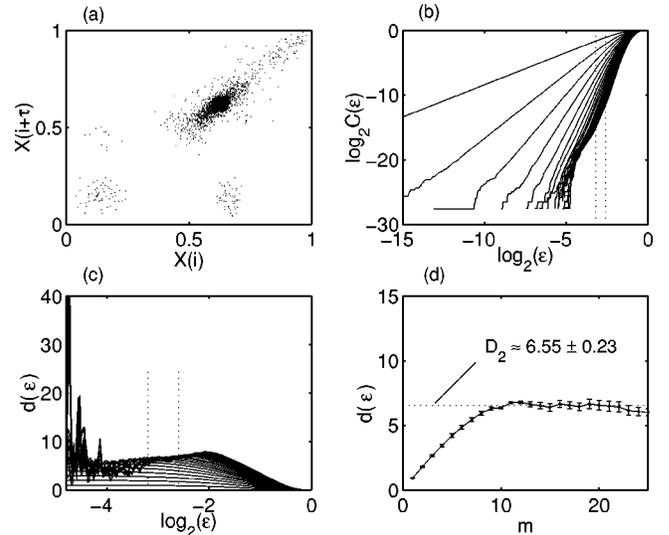

FIG. 1. (a) Phase portrait (delay time 6 s) for the principal components of FMRI data from the rest plus finger-tapping task, (b) $\log_2 C(\epsilon)$ vs $\log_2 \epsilon$, (c) Local slopes $[d(\epsilon)]$ vs $\log_2 \epsilon$ (a clear scaling behavior for $\epsilon\in[0.12,0.17]$, between two dotted lines), and (d) $d(\epsilon)$ vs m for $\epsilon\approx[0.12,0.17]$.

ance (the first component being excluded) in the dataset of each run. The first component was excluded because it represented the variance due to different brain tissues other than those involved in the functional dynamics, as revealed by the inspection of the image of the corresponding spatial mode. The extraction of useful principal components has the advantage of reducing both computational load and noise in the signals. Out of all the components (50×500 time points), with a separate time-delay embedding scheme, a phase space was reconstructed for embedding dimension (m) from 2 to 25. With the delay vectors constructed from 25 000 data points, one could estimate the correlation dimension as high as 10 if the scaling region occurs for $\epsilon\geq0.14$ [29]. Figure 1(a) shows a projection of 15-dimensional phase space onto two dimensions, constructed with a delay time of $6s$ from 50 principal components of the FMRI data collected from one subject doing the second task. We remark here that such a phase space constructed from multiple time series has disjoint sets and cannot be used to observe continuously evolving dynamics. However, the cross-correlation sum can still be calculated for such sets to a good precision and is essentially identical to their (auto) correlation sums above certain length scale [23]. The plot indicates nonlinearity in the data because the phase portrait is not symmetrical with respect to reflection in the diagonal line. In contrast, for a random process, the phase portrait would be symmetrical [30]. Figure 1(b) is a plot of $\log_2 C(\epsilon)$ vs $\log_2 \epsilon$ for the same data. The plot indicates power law behavior of the correlation sums with most of the length scale ϵ at all reconstructed phase space of dimensions $m=2$ to 25. A scaling behavior is apparent for $\epsilon\in[0.12,0.17]$ as shown in the plot of local slopes $[d(\epsilon)]$ vs $\log_2 \epsilon$ [Fig. 1(c)]. The size of this scaling region is about 5% of the maximum extent of the attractor. We can read off the values for D_2 at sufficiently high embedding dimension in this regime. Statistical fluctuations (dynamical complexity
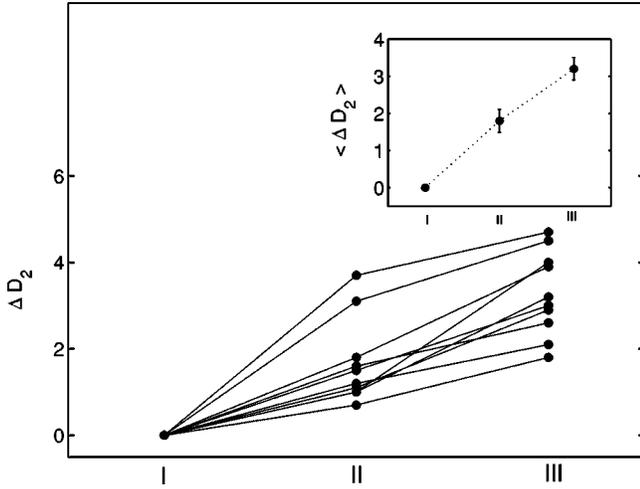
FIG. 2. The difference (ΔD_2) of correlation dimensions for the second and the third tasks with respect to the reference condition (rest): there are significant differences in the values of D_2 ($\langle \Delta D_2 \rangle$ $\pm$ standard error mean for (i) the second task: 1.80 ± 0.31 and (ii) the third task: 3.20 ± 0.30, shown in the inset). Note that all the subjects displayed monotonically increasing D_2 related to task difficulty (statistical significance, $p < 0.01$).

and noise) distort the scaling behavior below this length scale. At sufficiently high embedding dimensions, the values of D_2 estimated from this scaling region remained substantially the same [Fig. 1(d)].

Similarly, after establishing a scaling region in the graph of $d(\epsilon)$ and $m\rho(\epsilon)$ vs $\log_2 \epsilon$, we estimated correlation dimensions for all the subjects. We found that the correlation dimension changed significantly with the tasks: it was the highest for the calculation-finger-opposition task and the lowest for the reference task. Figure 2 summarizes the results of the changes (ΔD_2) with tasks for all the subjects. With ΔD_2, there is a significant dimension increase of 1.8 ± 0.3 (mean$\pm$standard error mean) from the first to the second task and 3.2 ± 0.3 from the first to the third. Figure 3 shows the comparison of three curves of $m\rho(\epsilon)$ vs $\log_2(\epsilon)$ for the tasks, rest (I), finger opposition (II), and finger opposition plus calculation (III) (calculated at $m = 20$). Also with $m\Delta\rho$, there is also an increase of 1.7 ± 0.3 from the first to the second task
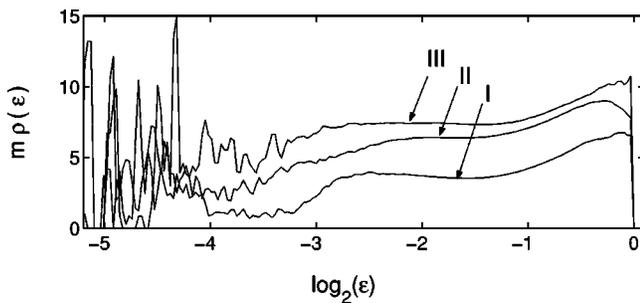

FIG. 3. For the three tasks (I=rest, II=finger opposition, and III=finger opposition plus calculation), the variation of $m\rho(\epsilon)$ with $\log_2(\epsilon)$. There is a significant difference of the values of $m\rho(\epsilon)$ at the scaling regions for the different tasks (these curves were calculated for $m = 20$).
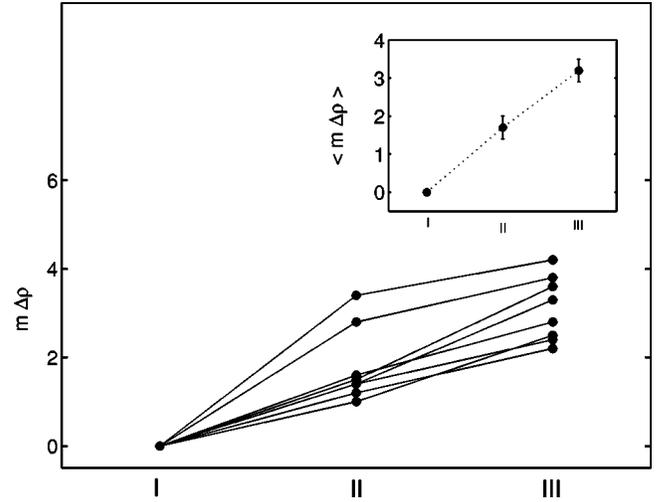

FIG. 4. The difference ($m\Delta\rho$) for the second and the third tasks with respect to the reference condition (rest): there are significant differences in the values of $m\rho$ ($\langle m\Delta\rho \rangle \pm$ standard error mean for (i) the second task: 1.70 ± 0.30 and (ii) the third task: 2.90 ± 0.20, shown in the inset)(statistical significance, $p < 0.01$).

and 2.9 ± 0.2 from the first to the third tasks, as shown in Fig 4. These results support the hypothesis that the correlation dimension of FMRI signals is higher in conditions that demand a greater mental effort.

In order to compare our results based on the concepts derived from the theory of nonlinear dynamics to linear analysis including conventional imaging analysis for neurophysiologists, we computed (i) the mean amplitude of the signals for all the tasks, (ii) the frequency power spectra of the signals, (iii) the number of correlated voxel pairs above certain threshold value of Spearman's correlation coefficients (to contrast GP algorithm that counts the pairs of delay vectors within ϵ radius), and performed a standard general linear model analysis with SPM99 [28], shown in Fig. (5). The mean amplitude changed approximately by 0.5% between the first and the second tasks, and by 1.0% between the first and the third tasks (statistical significance, $p < 0.10$). The power spectrum of the FMRI signals revealed a larger number of frequency peaks (or broader frequency band) for more difficult tasks [see Fig. 6(a) for all the tasks I–III in one subject]. Figures 6(b)(I–III) show average frequency spectrum of all the subjects. The average spectrum preserves the dominant frequency peaks at 0.05 and 0.1 Hz corresponding to the task cycles for the second and the third tasks. The number of correlated voxel pairs in the brain overall increased by 3% from the first to the second task ($p < 0.10$) and by 1% from the second to the third ($p < 0.10$). The general procedure for statistical parametric mapping analysis is described here. Following motion correction, the functional FMRI images were first spatially transformed into a commonly accepted brain coordinate system using a 12-parameter affine transformation followed by nonlinear wrapping. These images were spatially smoothed with an 8-mm isotropic Gaussian Kernel. Data were also bandpass filtered in the time domain to remove high-frequency noise and artifactual signal drifts. The statistical analysis was performed by modeling the two task
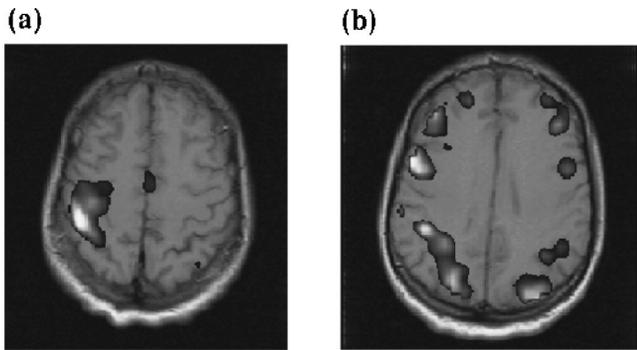
(a)   **(b)**

FIG. 5. The SPM analysis of the FMRI data collected during the rest-tapping and calculation-tapping tasks. The black and white spots inside the brain represent the significantly active voxels linearly correlated with the hypothesized response. This is a static measure of activity, shown for comparison with the dynamics results. (a) Tapping-vs-rest contrast, showing activated areas in the hand portion of the left primary sensorimotor cortex and in the supplementary motor area, and (b) calculation-vs-tapping contrast, showing several clusters of activations, located mostly in frontal, prefrontal, and posterior parietal cortices (the probability threshold set at $p < 0.05$, corrected for multiple comparisons).

conditions (finger tapping and calculation) as square waves convolved with a synthetic hemodynamic response function, which were entered as separate effects in the statistical design matrix. Figures 5(a) and 5(b) show the relative activations of brain areas in one subject during the second and third tasks in the tapping-vs-rest and calculation-vs-tapping contrasts, respectively. The finger-tapping task strongly activated the hand portion of the left primary sensorimotor cor-
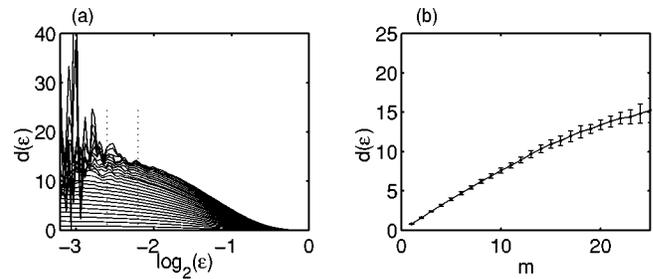

FIG. 7. For the multivariate surrogate data, (a) local slopes $d(\epsilon)$ vs $\log_2 \epsilon$: there is apparently no scaling region, and (b) $d(\epsilon)$ vs m for $\epsilon \approx [0.17, 0.22]$): there is no saturation of $d(\epsilon)$, shown for a region $\epsilon \approx [0.17, 0.22]$.

tex and the supplementary motor area. The calculation elicited additional activations in frontal and prefrontal cortex as well as in posterior parietal areas. This analysis indicates that a higher mental load may result in a more spatially distributed activation and may be associated with higher levels of independent neural processes.

Experimental measurements are never noise-free. This fact poses a concern for our calculation, which may be related to whether the results are due to correlated noise in the FMRI data. To test this null hypothesis that the results are due to stochastic fluctuations, we constructed a number of multivariate surrogate data from each data set by randomizing their phases in the Fourier domain (within the component and across components), but preserving their linear correlations [31,32]. The null hypothesis was rejected as there was apparently no scaling region with the surrogate data [see Figs. 7(a) and 7(b)]. This means that the deterministic part is
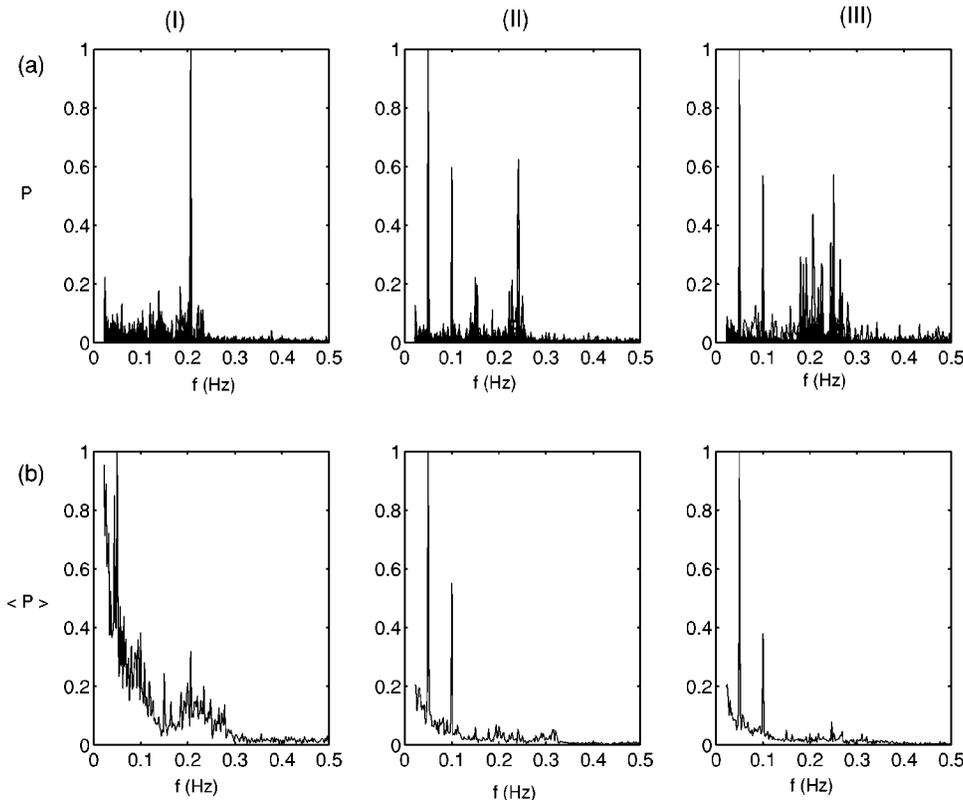

FIG. 6. Frequency spectrum (spectral power P in arbitrary units versus frequency, f, in Hz): (a) there are more peaks at higher frequencies for the third task (III) than for the second (II) or the first (I), and (b) the average spectrum for all the subjects preserves the dominant frequency peaks at 0.05 and 0.1 Hz corresponding to the task cycles of the second and the third tasks.

dominant in the FMRI signals. Successful estimates of correlation dimension indicate the presence of a dominant deterministic dynamical structure governing a complex system such as the human brain and are, therefore, reflective of the level of dynamical complexity in the FMRI signals.

IV. DISCUSSION: PHYSIOLOGICAL INTERPRETATIONS AND FUTURE CHALLENGES

Complex systems such as the human brain can be thought of as having enormous numbers of interrelated dependent variables. It may not be possible to measure all of them directly. It is, therefore, intuitive to take these dimension estimates from different experimental conditions in a relative sense. These results of increasing correlation dimension with increasing task load indicate that more mental activity involves a higher number of temporally independent processes contributing to the complexity of brain dynamics. The dynamic complexity of brain signals has been previously shown to correlate with the conscious state of the subject. For example, cerebral blood flow is globally reduced during slow-wave sleep as compared to both wakefulness and rapid eye movement sleep [9–11]. The differing dynamical complexities of the human brain can be understood as the results of differing numbers of temporally independent neuronal assemblies that may also be spatially distributed [33]. The higher value of the correlation dimension during the calculation task than during the other two tasks reflects the involvement of more neuronal assemblies contributing to more complex FMRI signals. Because these are spatially distributed networks, the increase in correlation dimension suggests that this increase in complexity changes the pattern of activity in both space and time. In effect, the brain uses more degrees of freedom to accomplish a task of greater complexity. This has important implications for the study of neural systems in humans.

Calculation of correlation dimensions provides us with useful measures as to how many order parameters to expect even when the system, like the human brain, is spatially extended, highly interconnected and very complex. However, the calculation always suffers from several experimental and theoretical limitations. For an exact determination of correlation dimension, the Grassberger-Procaccia algorithm requires a long enough noise-free time series under steady state conditions. Unfortunately, in practice, these conditions can never be fulfilled completely by physiological measurements, such as electroencephalography, magnetoencephalography, or FMRI. The calculation of dimension from brain signals is a compromise with the experimental measurement and also with the computational (i.e., size of the dataset) limitations (see also Refs. [34–36]). Thus, the results of successful dimensional estimates can be understood in a relative sense, for instance, to compare dynamical complexity in different situations. Given these limitations, we do not maintain that the absolute estimates of dimension reflect the true dimension of the brain. Even so, the relative measures are meaningful.

Although linear analysis is generally useful, the reliability of the analysis can be enhanced by the use of nonlinear techniques. Particularly, the nonlinear measures based on the correlation sum from the reconstructed phase space are reliably sensitive to the complexity of the signals compared to the linear measures. Although the precise nature of the signals that result in relative changes in these nonlinear measures needs more investigation, one can say that these measures are sensitive to changes in signal amplitude and frequency power spectrum. For example, let us consider two signals with different amplitudes A_1 and A_2. The correlation integral in GP algorithm measures the probability of finding a point pair inside a hypersphere of radius ϵ in a reconstructed space of dimension m and this probability is proportional to $(\epsilon/A_1)^m$ and $(\epsilon/A_2)^m$ for the two signals, respectively. The relative increase in correlation integral is thus on the order of $(A_2/A_1)^m$ (it is amplified in high-dimensional space). Even a simple change in amplitude can result in very noticeable change in correlation dimensional measures. The frequency of the signals can also affect these measures in very subtle ways: the probability measure for point pairs to fall within ϵ radius is overall greater for higher frequency signals.

In summary, our work suggests that the principal components of FMRI signals can be used to estimate the correlation dimension related to different behavioral tasks. In a relative sense, the correlation dimension estimates are useful dynamical complexity measures in evaluating the level of mental activity. The monotonic relationship of the correlation dimension with the behavioral tasks indicated that a higher mental load is associated with a higher dynamical complexity. These results indicate that higher mental activity involves a higher number of temporally independent neuronal processes contributing to complex brain dynamics. The findings suggest potential applications of the variation of the correlation dimension as a global measure of levels of brain activity. This applications of this measure may yield insight into the dynamic range of human intelligence and in characterizing certain mental disorders of brain function, like depression and schizophrenia. For example, the relationship of intelligence to brain function has been investigated with similar brain imaging techniques [37], suggesting that "general intelligence" is a function of frontal lobe activity. The aforementioned study examined static correlations of brain activity with measures of individual performance. Further work is warrrented to elucidate the relationship between spatial localization of brain activity and its dynamic complexity. We believe that bridging the measure of dynamic complexity with the spatial distribution of activity will ultimately yield insights not only into human intelligence but mental illness as well.

[1] Analyzing nonlinear time series is such a rich field that even a partial list of the relevant papers will be very long here. See, for example, H. Kantz and T. Schreiber, in *Nonlinear Time Series Analysis* (Cambridge University Press, Cambridge, UK, 1997), references therein.

[2] The reconstruction theorem applies also for spatiotemporal series. It can be inferred, for example, from the proof that the evolution described by an autonomous set of partial differential equations in a finite region of space asymptotically is confined to a finite-dimensional attractor [A. Debussche and M. Marion, J. Diff. Eqns. **100**, 173 (1992)].

[3] P. Grassberger and I. Procaccia, Phys. Rev. Lett. **50**, 346 (1983); Physica D **9**, 189 (1983).

[4] J. Martinerie, C. Adam, M. Le Van Quyen, M. Baulac, S. Clemenceau, B. Renault, and F.J. Varela, Nat. Med. **4**, 1173 (1998).

[5] D. Lerner, Physica D **97**, 563 (1996).

[6] W. Lutzenberger, H. Preissl, and F. Pulvermuller, Biol. Cybern. **73**, 477 (1995).

[7] J. Lamberts, P.L.C. van den Broek, L. Bener, J. van Egmond, R. Dirksen, and A.M.L. Coenen, Neuropsychobiology **41**, 149 (2000).

[8] I. Osorio, M.A. Harrison, Y.-C. Lai, and M. Frei, J. Clin. Neurophysiol. **18**, 269 (2001).

[9] G. Widman, T. Schreiber, B. Rehberg, A. Hoeft, and C.E. Elger, Phys. Rev. E **62**, 4898 (2000).

[10] A.R. Braun *et al.*, Science **279**, 91 (1998).

[11] P. Maquet *et al.*, Nature (London) **383**, 163 (1996).

[12] G. Tononi and G.M. Edelman, Science **282**, 1846 (1998).

[13] S. Ogawa, T.M. Lee, A.R. Kay, and D.W. Tank, Proc. Natl. Acad. Sci. U.S.A. **87**, 9868 (1990).

[14] K.K. Kwong *et al.*, Proc. Natl. Acad. Sci. U.S.A. **89**, 5675 (1992).

[15] D. Broomhead and G.P. King, Physica D **20**, 217 (1986).

[16] D. Broomhead, R. Jones, and G.P. King, J. Phys. A **20**, 563 (1987).

[17] E. Ott, T. Sauer, and J.A. Yorke, in *Coping with Chaos* (Wiley, New York, 1994).

[18] F. Takens, in *Dynamical Systems and Turbulence*, edited by D. Rand and L.S. Young, Lecture Notes in Mathematics Vol. 898 (Springer-Verlag, Berlin, 1981), p. 366; N.H. Packard, J.P. Crutchfield, J.D. Farmer, and R.S. Shaw, Phys. Rev. Lett. **45**, 712 (1980).

[19] T. Sauer, J.A. Yorke, and M. Casdagli, J. Stat. Phys. **65**, 579 (1991); Y.-C. Lai and D. Lerner, Physica D **115**, 1 (1998).

[20] M. Ding, C. Grebogi, E. Ott, T. Sauer, and J.A. Yorke, Physica D **69**, 404 (1993).

[21] B.B. Mandelbrot, in *The Fractal Geometry of Nature* (Freeman, San Francisco, 1982).

[22] J. Theiler, Phys. Rev. A **34**, 2427 (1986).

[23] H. Kantz, Phys. Rev. E **49**, 5091 (1994).

[24] A. Celletti, V.M.B. Lorenzana, and A.E.P. Villa, J. Stat. Phys. **89**, 877 (1997).

[25] M. Dhamala, Y.-C. Lai, and E. J. Kostelich, Ph.D. thesis University of Kansas, USA, 2000; M. Dhamala, Y.-C. Lai, and E.J. Kostelich, Phys. Rev. E **64**, 056207 (2001). The main point of the reference is that the GP algorithm is equally applicable to estimate the correlation dimension from an ensemble of short chaotic transients. This is based on the natural measure of chaotic saddle that can be obtained by a large number of chaotic transients.

[26] J.-P. Lachaux, L. Pezard, L. Garnero, C. Pelte, B. Renault, F.J. Varela, and J. Martinerie, Hum. Brain Mapp **5**, 26 (1997).

[27] C. Raab and J. Kurths, Phys. Rev. E **64**, 016216 (2001).

[28] Statistical parametric mapping refers to the construction and assessment of spatially extended statistical process and is used to test hypotheses about brain imaging data. These ideas have been instantiated in software that is called SPM. This software package performs statistical parametric mapping on a voxel-wise basis across the entire dataset with the assumption that image sources are independent. It is specifically designed for fitting general linear models of experimentally controlled variables to the measured data. (The internet site for this software package is http://www. fil.ion.ucl.ac.uk/spm.) [K.J. Friston *et al.*, Neuroimage **10**, 1 (1999).]

[29] For reliable dimension estimation, the minimal number of data points N required are given by $N > \epsilon^{-D_2/2}$, where ϵ is the scaling region in units of the diameter of the reconstructed attractor [J.-P. Eckmann and D. Ruelle, Physica D **56**, 185 (1992)].

[30] A.J. Lawrence, Int. Statist. Rev. **59**, 67 (1991).

[31] D. Prichard and J. Theiler, Phys. Rev. Lett. **73**, 951 (1994).

[32] S.J. Schiff and T. Chang, Biol. Cybern. **67**, 387 (1992).

[33] J.A.S. Kelso, in *Dynamic Patterns: The Self-Organization of Brain and Behavior* (MIT Press, Cambridge, MA, 1999).

[34] P.E. Rapp, T.R. Bashore, J.M. Martinerie, A.M. Albano, I.D. Zimmerman, and A.I. Mees, Brain Topogr. **2**, 99 (1989).

[35] A. Babloyantz, C. Nicolis, and M. Salazar, Phys. Lett. A **111**, 152 (1985).

[36] G. Mayer-Kress (Editor), in *Dimensions and Entropies in Chaotic Systems* (Springer-Verlag, Berlin, Germany, 1986).

[37] J. Duncan, F.J. Seitz, J. Kolodny, D. Bor, H. Herzog, A. Ahmed, F.N. Newell, and H. Emslie, Science **289**, 457 (2000).